

# Difference of Potential Range Formed at the Anode Between Water Drop Test and Temperature Humidity Bias Test to Evaluate Electrochemical Migration of Solders for Printed Circuit Board

Young Ran Yoo and Young Sik Kim<sup>†</sup>

*Materials Research Centre for Energy and Clean Technology, Department of Materials Science and Engineering,  
Andong National University, 1375 Gyeongdong-ro, Andong, Gyeongbuk, 36729, Korea*  
(Received June 06, 2023; Revised June 20, 2023; Accepted June 20, 2023)

Two types of accelerated tests, Water Drop Test (WDT) and Temperature-Humidity-Bias Test (THBT), can be used to evaluate the susceptibility to electrochemical migration (ECM). In the WDT, liquid water is directly applied to a specimen, typically a patterned conductor like a printed circuit board. Time to failure in the WDT typically ranges from several seconds to several minutes. On the other hand, the THBT is conducted under elevated temperature and humidity conditions, allowing for assessment of design and life cycle factors on ECM. THBT is widely recognized as a more suitable method for reliability testing than WDT. In both test methods, localized corrosion can be observed on the anode. Composition of dendrites formed during the WDT is similar to that formed during THBT. However, there is a lack of correlation between the time to failure obtained from WDT and that obtained from THBT. In this study, we investigated the relationship between electrochemical parameters and time to failure obtained from both WDT and THBT. Differences in time to failure can be attributed to actual anode potential obtained in the two tests.

**Keywords:** Printed circuit board, Solder, Electrochemical Migration, Pitting potential, Protection potential

## 1. Introduction

ECM is the phenomenon characterized by the formation of conductive metal filaments on a printed circuit board (PCB) under the influence of a DC voltage bias [1]. These filaments can grow on the external surface, internal interfaces, or within the bulk material of a composite (e.g., paper/phenolic laminate) [2,3]. The growth of metal filaments occurs through electrodeposition from a solution containing metal ions that dissolve from the anode, are transported by the electric field, and then re-deposited at the cathode. It's important to note that this definition excludes other phenomena such as field-induced metal transport in semiconductors and the diffusion of corrosion by-products. Surface Insulation Resistance (SIR) testing has been employed in the electronics industry since the introduction of transistors and printed circuit boards [4-10].

The WDT refers to a test where an electrical potential is applied to two adjacent unprotected metal patterns

under ambient conditions. A drop of deionized water is then applied to the sample, bridging the two conductors. The THBT regimen involves subjecting a material or materials system to elevated temperature and humidity conditions for a specified duration, beyond ambient conditions. Additionally, an electrical potential is applied between adjacent electrodes of the test patterns. The applied potential level, duration, and the point at which it is applied can vary.

To evaluate susceptibility to ECM, two types of accelerated tests are commonly used: the WDT and the THBT. In the WDT, a drop of liquid water is directly applied to a specimen, typically a patterned conductor like a printed circuit board. The time to failure usually ranges from several seconds to several minutes. However, reproducibility issues have been reported in previous WDT studies due to the current's strong dependence on the droplet's size and shape. On the other hand, the THBT is performed under elevated temperature and humidity conditions. The effectiveness of design and lifecycle factors on ECM can be used to evaluate. Therefore, the THBT is widely considered more suitable for reliability

<sup>†</sup>Corresponding author: [yikim@andong.ac.kr](mailto:yikim@andong.ac.kr)  
Young Ran Yoo: Ph.D. Senior Researcher, Young Sik Kim: Professor

testing compared to the WDT. The time to failure in THBT typically ranges from several hours to thousands of hours.

Various researchers have proposed mechanisms for electrochemical damage in electronic components. According to Takemoto, the following factors contribute to the occurrence of ECM: 1) the rate of metal ion leaching, 2) the lower the hydrogen evolution, which is a competing reaction in cathodic reduction, and 3) the faster precipitation due to a lower saturation concentration of metal ions [11]. Radovici also reported that the dissolution rate at the anode facilitates migration [12]. Tanaka's research found that Pb-free solder exhibits increased ECM resistance compared to SnPb solder due to the formation of a more stable passive state by Sn than Pb [13].

The addition of alloying elements can affect the ECM resistance of solder alloys. Alloying elements such as Ag, Cu, In, Zn, and Bi have been reported to influence the dissolution behavior at the anodes, thereby changing the corrosion resistance and ECM susceptibility of solders [7,13-16]. Additionally, many researchers have reported that test environmental such as temperature, humidity, contaminants have effects on ECM and corrosion of lead-free solder alloys [5,8-10,17,18]. High corrosion resistance of solder alloys to reduce ECM susceptibility [19-21]. The applied voltage also has a significant influence on resistance to ECM. The applied voltage also has a significant influence on resistance to ECM, the higher the applied voltage, the shorter the time-to-failure if the spacing between the two electrodes is fixed [15,22,23]. Additionally, Osman et al. reported that ECM resistance has been reported to be related to corrosion potential, pitting potential, passivation potential and corrosion current density in the electrochemical polarization behavior that used to evaluate corrosion resistance [8-10,19-21,24-26].

These studies do not satisfy all correlations with polarization behavior of solder alloys by various ECM evaluation methods. Therefore, in this study, we preferred the WDT and the THBT specimens of pure Sn, Sn37Pb, Sn3.5Ag, Sn3.0Ag0.5Cu, and Sn58Bi solders. We evaluated the time to failure using both the WDT and THBT methods and performed polarization tests on these solder alloys. Additionally, we compared the time to failure with the electrochemical parameters obtained from

the anodic polarization and reverse polarization curves. In this work, the effect of the anode potential according to the accelerated ECM evaluation method of solder alloy was examined.

## 2. Experimental Methods

### 2.1 Experimental solder alloys

In this study, pure Sn, Sn37Pb, Sn3.5Ag, Sn3Ag0.5Cu, and Sn58Bi solders were used. The specimen used for the WDT was prepared on a Si wafer substrate. On the p-type <100> Si wafer substrate, a Ni under bump metallurgy (UBM) layer was sputtered with a thickness of 3000 Å. A pad with a 300 µm spacing pattern was created using the photo-resist and screen printing methods. For the THBT, PCB specimens were utilized, with a total of 10 specimens. The THBT was conducted following the guidelines of IPC-TM-650 2.6.14.1 ECM Resistance Test [27].

### 2.2 Water Drop Test

To evaluate the resistance to ECM, the WDT [5,8,12,13] was used. The specimen used in the WDT was fabricated on a Si wafer substrate. A Ni UBM with a thickness of 3000 Å was sputtered onto the Si wafer substrate. A pad with a spacing pattern of 300 µm was created using the screen printing and photo-resist methods. Solder pastes were reflowed onto the Ni UBM using a reflow oven. Following the reflow process, the specimen was annealed for 5 hours at 150 °C to minimize the phase transformation between the Ni UBM and solder alloy.

The WDT was conducted to investigate the failure mechanism in the pad-patterned solder alloy when exposed to 0.001 wt% NaCl and 0.001 wt% Na<sub>2</sub>SO<sub>4</sub> solutions at room temperature. A micro syringe was used to dispense 2 µL of the test solution between the pad-patterned solders, and a DC voltage of 2 V was applied using a potentiostat (model 273A, EG&G, USA) as the DC power source. The current or resistance were measured, and continuous video and images of the migration process were recorded using a video-microscope [1,8,9].

### 2.3 Temperature-Humidity-Bias Test

The THBT was conducted on a PCB (FR-4) substrate.

Which a 400  $\mu\text{m}$  space pattern for the ECM experiments with solder alloys. The PCB substrate had a Cu UBM that was electroless plated with a thickness of approximately 2 ~ 3  $\mu\text{m}$ . A comb line pattern with a 400  $\mu\text{m}$  spacing was created using photo-resist techniques. To prevent solder adhesion in unintended areas, a photo-imageable solder resist (PSR) method was employed to coat the surface electric circuit lines. Subsequently, solder pastes were reflowed on the Cu UBM using a reflow oven.

THBTs were performed to gain insights into the failure mechanisms within a real PCB system. The test involved various solders, including pure Sn, Sn37Pb, Sn3.5Ag, Sn3Ag0.5Cu, and Sn58Bi. For each solder type, 10 testing specimens were used. A multi-specimen THBT system was developed using a switch module (Keithley 7001, SMU Instruments, USA). A constant DC voltage was applied to the specimens, and the current and resistance was measured using a source-meter (Keithley 2400, SMU Instruments, USA) between patterns. The time taken for surface insulation breakdown was measured at room temperature over a period of 96 hours under a 10 V bias. Subsequently, the testing chamber was set to a temperature of 85 °C and a relative humidity of 90%. DC voltage was applied to 40 specimens (across 4 channels) for 168 hours, and the current / resistance were measured in real-time.

#### **2.4 Polarization test**

The specimen used for the polarization test was prepared from a Ni-electroplated copper plate. The Ni-electroplated copper plate was cut into 1 cm  $\times$  1 cm specimens, and solder pastes were reflowed and annealed for 5 hours at 150 °C. The specimens were then polished using 0.05  $\mu\text{m}$  alumina paste. A coated lead wire was connected to the specimens, and the polished reflowed surface was sealed with epoxy resin exposure area: 0.09 cm<sup>2</sup>. Anodic polarization tests were evaluated in deaerated NaCl and Na<sub>2</sub>SO<sub>4</sub> solution at 25 °C using a Potentiostat (model DC105, Gamry, USA). The test solution was deaerated using N<sub>2</sub> gas for 30 minutes at a flow rate of 100 mL/min. A reference electrode was used as an SCE (saturated calomel electrode) and a counter electrode was used as a high-density graphite rod. The scanning rate was set at 1 mV/sec.

#### **2.5 Cyclic Polarization Test**

The specimens were polished using 1  $\mu\text{m}$  alumina paste. A coated lead wire was connected to the specimens, and the surface was sealed with epoxy resin, exposure area: 0.16 cm<sup>2</sup>. Cyclic polarization tests were evaluated in deaerated NaCl and Na<sub>2</sub>SO<sub>4</sub> solutions at 25 °C using a potentiostat (model DC105, Gamry, USA). The protection potential was determined through the cyclic polarization test.

#### **2.6 Surface analysis**

After the WDT and THBT, the specimens were left to dry naturally. Subsequently, the specimens were transferred to a SEM (Scanning Electron Microscope) chamber. The images of the anodic electrode and dendrite were observed using SEM and the composition of the dendrite were analyzed using EDS (Energy Dispersive X-ray Spectrometer) (JEOL, model JSM-6300, USA).

### **3. Results**

Two types of electrochemical tests commonly employed to assess ECM susceptibility are the WDT and the THBT. In the WDT, water is dropped onto a pad-patterned specimen, and when a DC voltage is applied, insulation breakdown occurs, yielding the time to failure. Typically, the time to failure in the WDT ranges from several seconds to several minutes. In contrast, the THBT is performed under high temperature and high humidity conditions. This test is well-known for evaluating ECM susceptibility and quantitatively determining the effects of ECM initiation, growth, and their dependence on various factors. Consequently, the THBT is considered more suitable than the WDT. The time to failure in the THBT ranges from several hours to thousands of hours.

Fig. 1 and 2 shows the morphology and composition of dendrites formed by the WDT and THBT. Dendrites formed by both test methods exhibit similar shapes regardless of the specific test employed. EDS-mapping analysis revealed that the primary elements constituting the dendrites were a mixture of Sn and Pb in the Pb-rich phase for Sn37Pb, while Sn constituted the dendrites for Sn58Bi. These results indicate that the WDT and THBT yielded consistent outcomes, with the dendrite compositions showing similar tendencies irrespective of the corrosive environment.

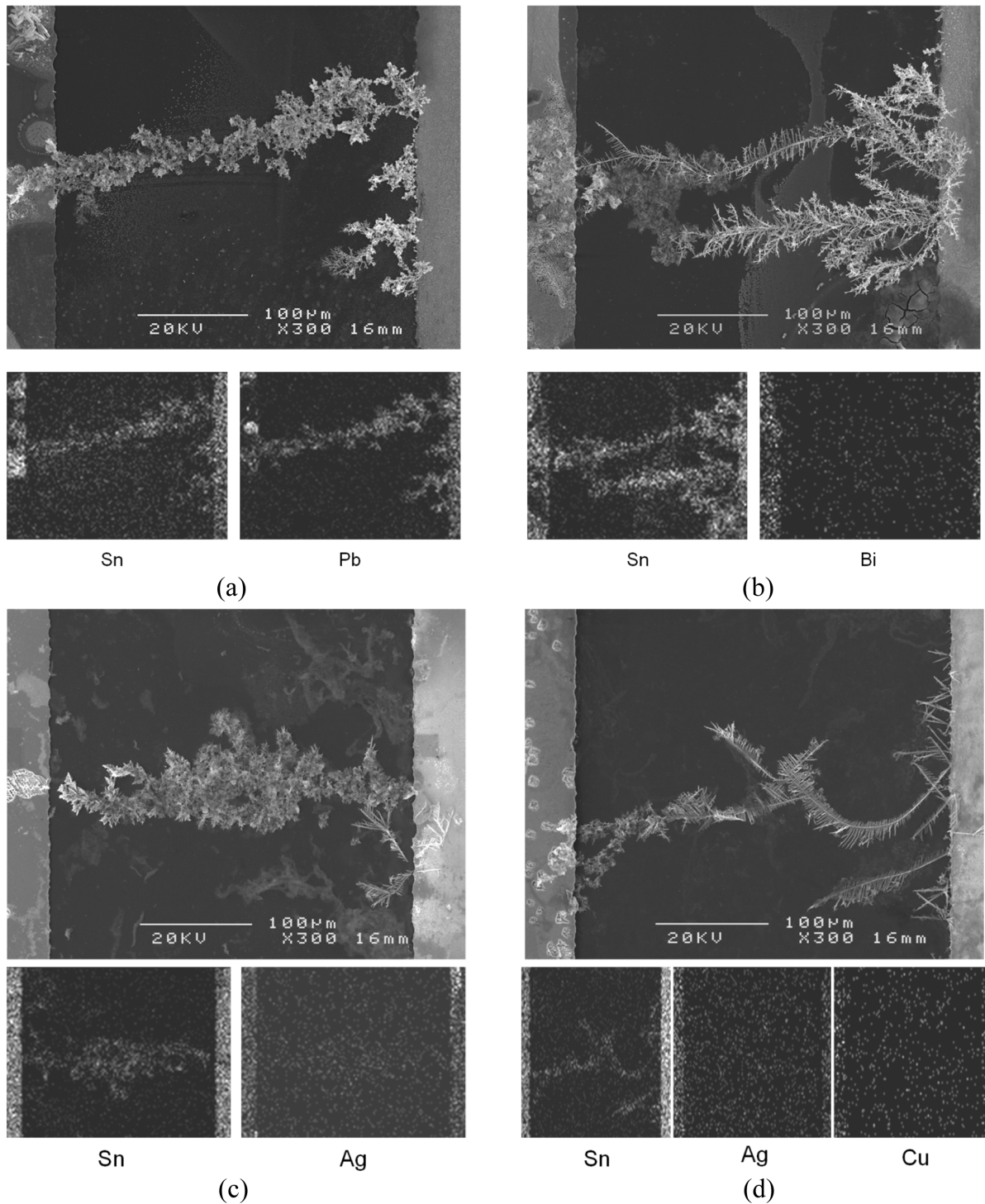


**Fig. 1. Morphology and composition of dendrite formed by the WDT for (a) Sn<sub>37</sub>Pb, (b) Sn<sub>58</sub>Bi, (c) Sn<sub>3.5</sub>Ag, (d) Sn<sub>3</sub>Ag<sub>0.5</sub>Cu solder alloys [(a)(b) Ref.5, Publication permission from Springer]**

The correlation between the time to failure results obtained from the WDT and THBT was compared. Fig. 3 illustrates the correlation between the time to failure determined by the WDT and that measured by the THBT

in a Cl<sup>-</sup> environment. The results indicate no significant correlation between the time to failure obtained from both test methods. This same observation was made when comparing the time to failure obtained from the WDT

DIFFERENCE OF POTENTIAL RANGE FORMED AT THE ANODE BETWEEN WATER DROP TEST AND TEMPERATURE HUMIDITY BIAS TEST TO EVALUATE ELECTROCHEMICAL MIGRATION OF SOLDERS FOR PRINTED CIRCUIT BOARD

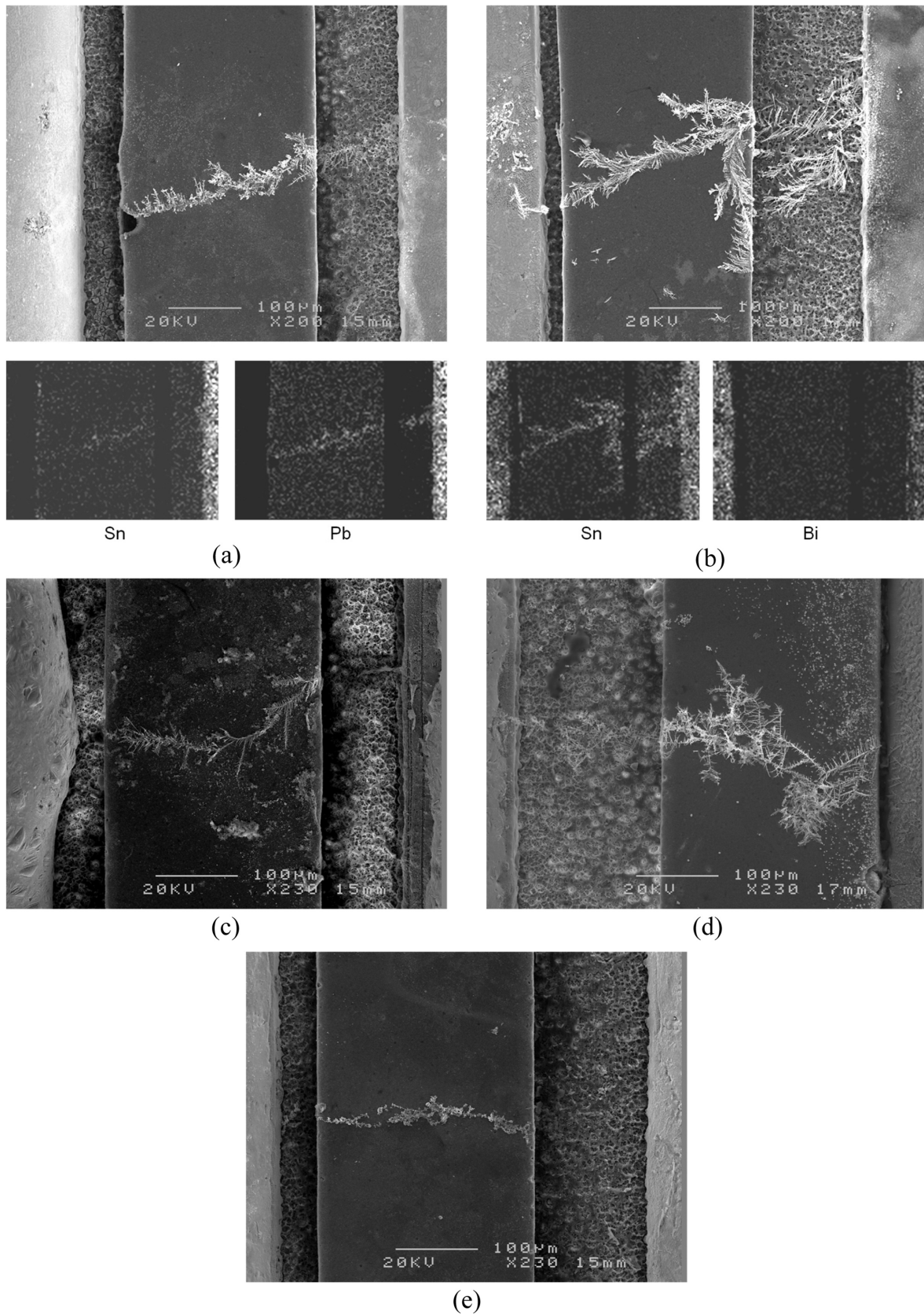
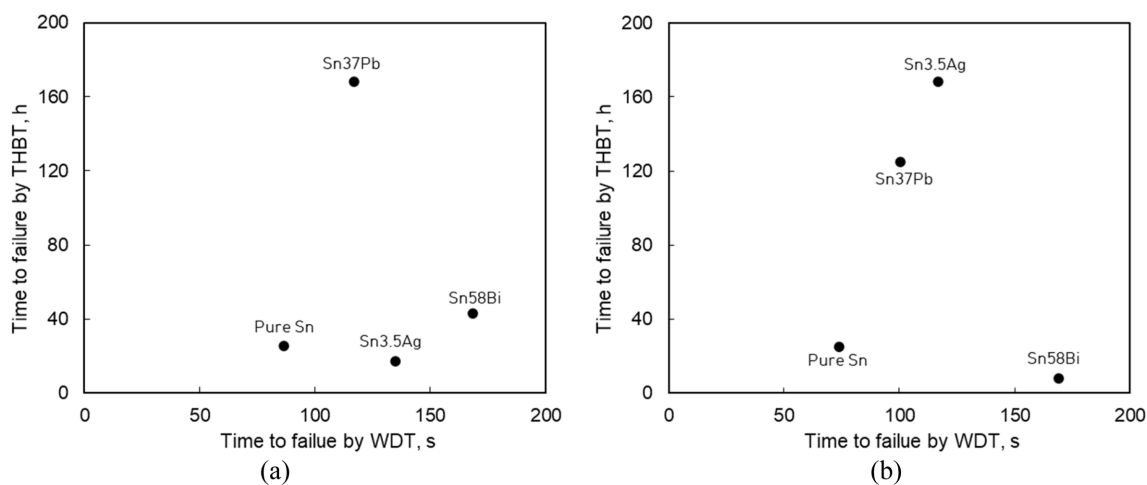
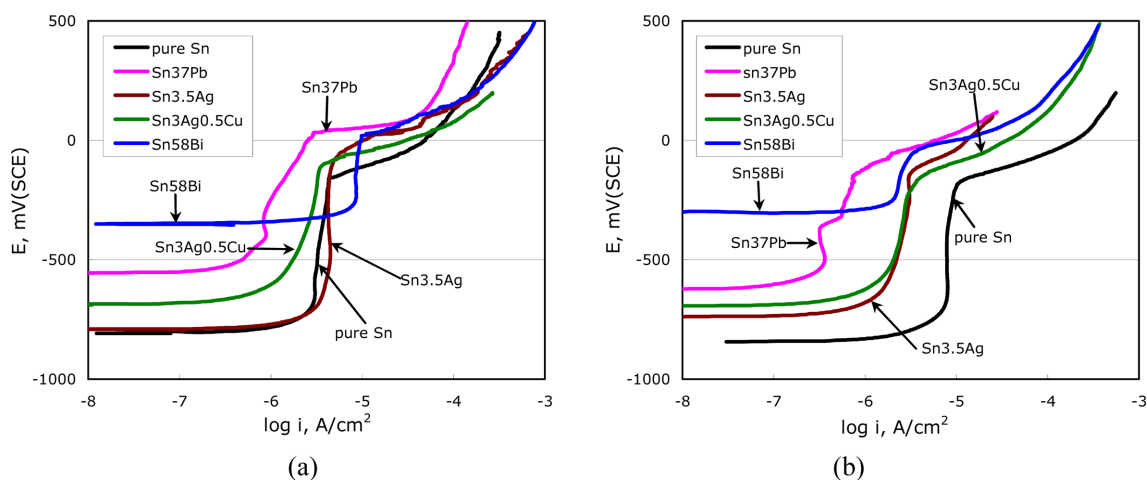


Fig. 2. Morphology and composition of dendrite formed by the THBT for (a) Sn37Pb, (b) Sn58Bi, (c) pure Sn, (d) Sn3.5Ag, (e) Sn3Ag0.5Cu solder alloys



**Fig. 3. Relationship between the averaged time to failure by the WDT and the THBT (a) in 0.001 wt% NaCl solution, (b) in 0.001 wt% Na<sub>2</sub>SO<sub>4</sub> solution**



**Fig. 4. Anodic polarization behavior of solder alloys (a) in deaerated 0.001 wt% NaCl at 25 °C, (b) in deaerated 0.001 wt% Na<sub>2</sub>SO<sub>4</sub> at 25 °C**

and THBT in an SO<sub>4</sub><sup>2-</sup> environment. ECM phenomena occur as a result of electrochemical processes. Therefore, to elucidate the causes of the differences in test results, polarization behavior of the solder alloys in each environment was examined.

ECM phenomena occur as a result of electrochemical processes. Therefore, to identify the causes of differences in test results, we examined the polarization behavior of the solder alloys in each environment. Fig. 4a presents the anodic polarization behavior obtained in a 25 °C, deaerated 0.001% NaCl environment, while Fig. 4b shows the anodic polarization behavior obtained in a 25 °C, deaerated 0.001% Na<sub>2</sub>SO<sub>4</sub> environment. We examined the

relationship between the parameters obtained from the polarization curves in each environment and the time to failure measured in the WDT and THBT.

The relationship between the parameters obtained from the polarization curves in each environment and the time to failure measured in the WDT and THBT is summarized in Table 1. The time to failure measured by the WDT showed a close correlation with the pitting potential ( $E_p$ ) in the polarization curves, regardless of the environment. However, the time to failure measured by the THBT exhibited a lower correlation with various electrochemical factors (corrosion current density,  $i_R$ , corrosion potential,  $E_R$ , passive current density,  $i_p$ ), including the pitting

**Table 1. Summary of relationships between the averaged time to failure ( $T_f$ ) by WDT and THBT and electrochemical parameters**

Time to failure	Environments	$E_R$		$i_R$		$E_p$		$i_p$	
		Cl <sup>-</sup>	SO <sub>4</sub> <sup>2-</sup>						
$T_f$ by WDT		○	△	×	△	○	○	×	×
$T_f$ by THBT		×	×	×	○	×	×	×	×

Remarks: Relationship between parameters - ○ close, △ medium, × low

potential in the polarization curves.

Therefore, through the analysis of the test conditions for each method, we aimed to compare the differences between the two test methods and investigate the causes using electrochemical analysis.

#### 4. Discussion

The conditions for the two test methods are presented in Table 2, revealing the following differences between the evaluation methods. The test solutions are the same, but the quantity of electrolyte used in the evaluation significantly differs, with the WDT employing a relatively larger amount in the WDT, when a voltage of 2 V was applied between the two terminals, the actual potential

formed was measured using a microprobe. Regardless of the solder and environment, the anode exhibited a potential of approximately -0.1 to +0.1 V (SCE), while the cathode showed a potential of approximately -2.2 to

**Table 2. Test Conditions of the WDT and the THBT**

Conditions	WDT	THBT
Test Solution	NaCl, Na <sub>2</sub> SO <sub>4</sub>	NaCl, Na <sub>2</sub> SO <sub>4</sub>
Thickness of water film	R.T., drop (2 $\mu$ L) <i>ca.</i> 500 $\mu$ m	85 °C, 90%RH < 10 $\mu$ m
Distance between electrodes	300 $\mu$ m	400 $\mu$ m
Applied Voltage	Low (2 V)	High (10 V)
Potential	0 V (anode) -2 V (cathode)	unknown

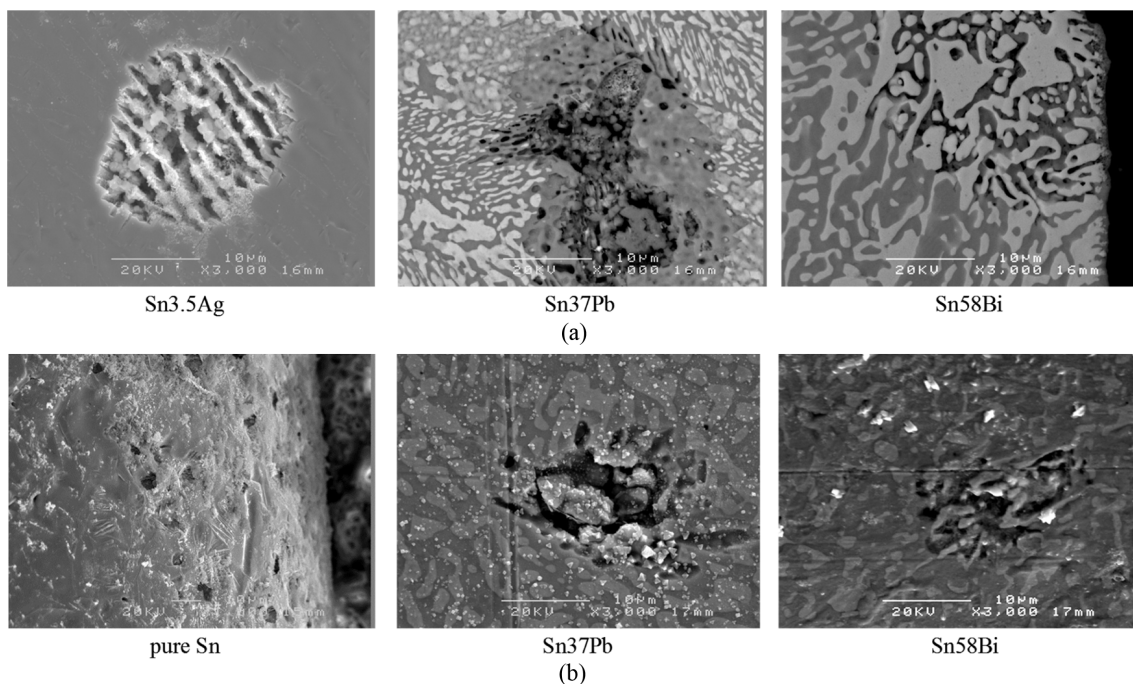


**Fig. 5. Occurrence of localized corrosion on the anode in the environment (a) after the WDT and (b) after the THBT [(a) Ref.5, Publication permission from Springer]**

-1.8 V (SCE). On average, the potential formed at the anode was defined as approximately 0 V (SCE), and it can be observed that the time to failure obtained from the WDT evaluation aligns well with the polarization behavior within the range of 0 V (SCE). However, in the case of the THBT, which forms a very thin electrolyte film, it is difficult to directly observe the anode potential formation due to challenges in applying a microprobe. The formation of an anode potential corresponding to the electrolyte film occurs at a lower potential than the formal potential when higher voltages are applied, potentially within the passive region. Upon visual inspection of the corrosion morphology at the anode using SEM after the actual tests (Fig. 5), it was observed that regardless of the

test method, the anode exhibited localized corrosion. This corrosion morphology indicates that the anode potential formed in the THBT may reside within the passive region but potentially at higher potentials within the passive region. Therefore, the correlation between the protection potential obtained from cyclic polarization behavior and the time to failure obtained from the THBT was examined.

Fig. 6 displays the cyclic polarization behavior of various solders in deaerated 0.001 wt% NaCl and Na<sub>2</sub>SO<sub>4</sub> solutions at 25 °C. The protection potential, defined as the potential where the reverse scan curve intersects the passive current curve in the cyclic polarization test, indicates the range where pitting corrosion can occur in the passive state. Fig. 7 illustrates the relationship between

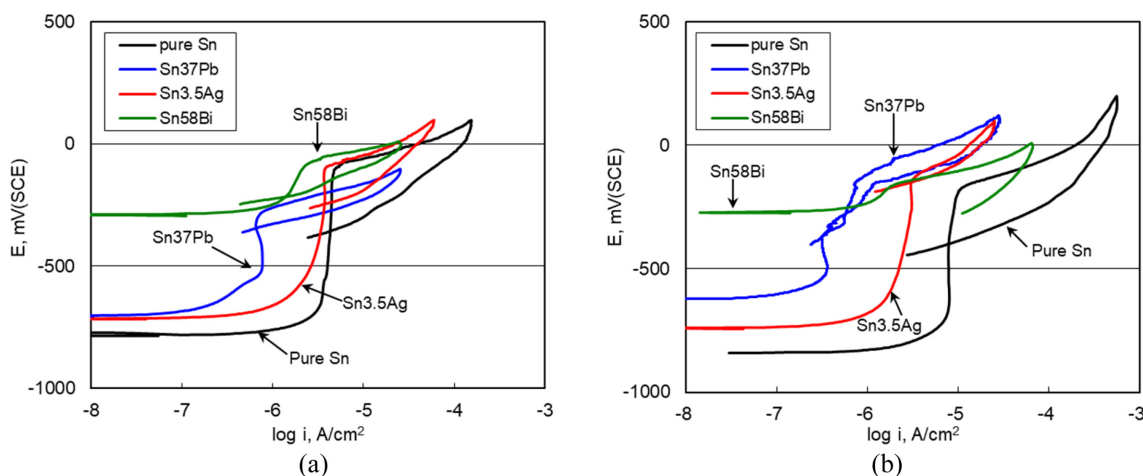


**Fig. 6.** Reverse polarization behavior of several solders obtained (a) in deaerated 0.001 wt% NaCl at 25 °C, (b) in deaerated 0.001 wt% Na<sub>2</sub>SO<sub>4</sub> at 25 °C

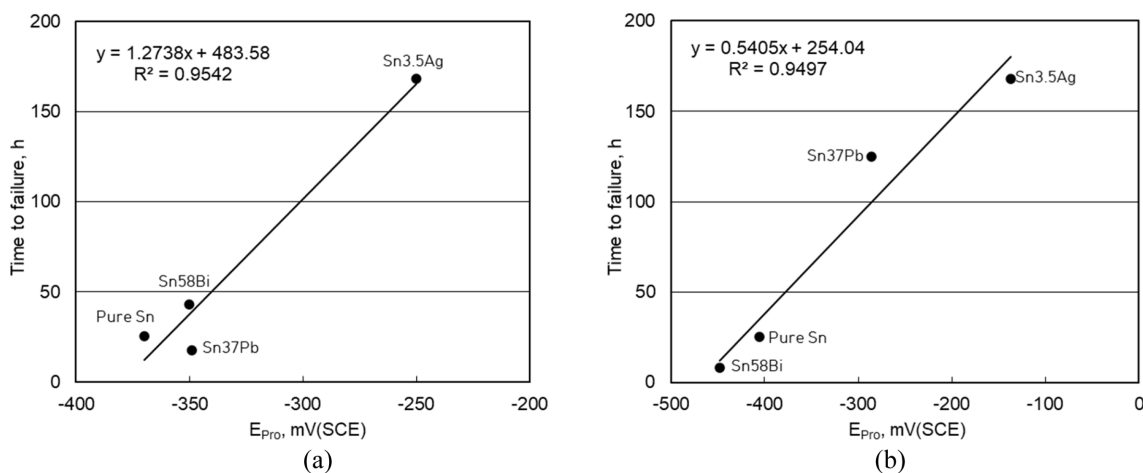


**Fig. 7.** Relationship between the averaged time to failure and protection potential obtained from cyclic polarization curves at 25 °C; (a) deaerated 0.001 wt% NaCl, (b) deaerated 0.001 wt% Na<sub>2</sub>SO<sub>4</sub>

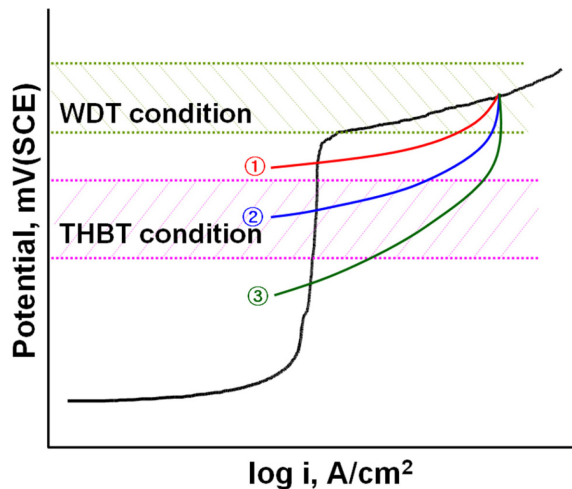


Fig. 8. Interpretation model on the difference of the time to failure between WDT and THBT

the time to failure and the protection potential obtained from the cyclic polarization curves at 25 °C: (a) for deaerated 0.001 wt% NaCl, and (b) for deaerated 0.001 wt% Na<sub>2</sub>SO<sub>4</sub>. Regardless of the corrosion environment, a good linear relationship exists between the protection potential and the time to failure. Reliability is also very high. This means that the ECM susceptibility determined by the THBT may be influenced by the protection potential of the solder.

Hence, this study proposes a new interpretation of the relationship between electrochemical parameters and ECM susceptibility obtained through the WDT and THBT. Fig. 8 shows an interpretation model for the difference in the time to failure by the test methods for assessing ECM susceptibility. The reason why the experimental results from the WDT and THBT do not align well is as follows: in the case of the WDT, the presence of a corrosive environment leads to the formation of an anode potential that exceeds the pitting potential, while in the THBT, the formation of a very thin water film on the surface results in an anode potential below the pitting potential but above the protection potential. Therefore, due to the difference in anode potential formation between the two test methods, the destructive tendencies obtained may not coincide, and the corrosion morphology at the anode indicates localized corrosion. Furthermore, in practical applications, the corrosive environment is expected to be milder than that in the THBT, so caution should be exercised when applying

ECM resistance determined by the THBT to actual conditions, as the anode potential formed would likely correspond to potentials above the natural potential.

## 5. Conclusions

This work performed both WDT and THBT using the specimens of pure Sn, Sn37Pb, Sn3.5Ag, Sn3.0Ag0.5Cu, and Sn58Bi solders in NaCl and Na<sub>2</sub>SO<sub>4</sub> environments. The followings were concluded.

The discrepancy between the results from WDT and THBT was obtained. In the case of WDT, a sufficiently corrosive environment exists, which leads to the formation of an anodic potential higher than pitting potential of the solders. However, in the case of THBT, because the water film is very thin, an anode potential was lower than the pitting potential, which was closely related to protection potential of the solders.

There existed a difference in anode potential formed between the test methods, which leads to the non-coincidence of the damage trends obtained from the WDT and the THBT.

## References

1. IPC-TR-476A, Electrochemical Migration: Electrically Induced Failures in Printed Wiring Assemblies, <http://ipc.org> (1997).
2. M. Jellesen D. Minzari, U. Rathinavelu, P. Møller, R. Ambat, Investigation of Electronic Corrosion Mechanisms, *ECS Transactions*, **25**, 1 (2010). Doi: <https://doi.org/10.1149/1.3321952>
3. Y. R. Yoo, Ph.D. Dissertation, pp. 41 - 43, Andong National University, Andong (2007).
4. S. B. Lee, Y. R. Yoo, J. Y. Jung, Y. B. Park, Y. S. Kim, and Y. C. Joo, *Proc. 56th Electronic Components and Technology Conf.*, p. 621, IEEE, San Diego, CA (2006). Doi: <https://doi.org/10.1109/ECTC.2006.1645714>
5. Y. R. Yoo and Y. S. Kim, Influence of Corrosion Properties on Electrochemical Migration Susceptibility of SnPb Solders for PCBs, *Metals and Materials International*, **13**, 129 (2007). Doi: <https://doi.org/10.1007/BF03027563>
6. S. B. Lee, Y. R. Yoo, J. Y. Jung, Y. B. Park, Y. S. Kim, and Y. C. Joo, Electrochemical migration characteristics of eutectic SnPb solder alloy in printed circuit board,

- Thin Solid Films*, **504**, 294 (2006). Doi: <https://doi.org/10.1016/j.tsf.2005.09.022>
7. Y. R. Yoo, H. S. Nam, J. Y. Jung, S. B. Lee, Y. B. Park, Y. C. Joo, and Y. S. Kim, Effects of Ag and Cu additions on the electrochemical migration susceptibility of Pb-free solders in Na<sub>2</sub>SO<sub>4</sub> solution, *Corrosion Science and Technology*, **6**, 50 (2007). <https://koreascience.kr/article/JAKO200721161743116.page>
  8. S. B. Lee, J. Y. Jung, Y. R. Yoo, Y. B. Park, Y. S. Kim, Y. C. Joo, Effect of applied voltage bias on electrochemical migration in eutectic SnPb solder alloy, *Corrosion Science and Technology*, **6**, 282 (2007). [https://www.j-cst.org/opensource/pdfjs/web/pdf\\_viewer.htm?code=C00060600282](https://www.j-cst.org/opensource/pdfjs/web/pdf_viewer.htm?code=C00060600282)
  9. Y. R. Yoo and Y. S. Kim, Influence of electrochemical properties on electrochemical migration of SnPb and SnBi solders. *Metals and Materials International*, **16**, 739 (2010). Doi: <https://doi.org/10.1007/s12540-010-1007-6>
  10. Y. R. Yoo and Y. S. Kim, Elucidation of the Relationship between the Electrochemical Migration Susceptibility of SnPb Solders for PCBs and the Composition of the Resulting Dendrites, *Metals and Materials International*, **16**, 613 (2010). Doi: <https://doi.org/10.1007/s12540-010-0814-0>
  11. T. Takemoto, R. M. Latanision, T. W. Eagar and A. Matsunawa, Electrochemical migration test of solder alloys in pure water, *Corrosion Science*, **39**, 1415 (1997). Doi: [https://doi.org/10.1016/S0010-938X\(97\)00038-3](https://doi.org/10.1016/S0010-938X(97)00038-3)
  12. O. Radovici and B. Popescu, Corrosion and Passivity of Some Pb-Sn Alloys in Media of Different pH, *Revue Roumaine de Chimie*, **15**, 1799 (1970).
  13. H. Tanaka, Factors leading to ionic migration in lead-free solder, *ESPEC Technology Report*, **14**, 1 (2002).
  14. J. Y. Jung, S. B. Lee, H. Y. Lee, Y. C. Joo and Y. B. Park, Electrochemical migration characteristics of eutectic Sn-Pb solder alloy in NaCl and Na<sub>2</sub>SO<sub>4</sub> solutions, *Journal of Electronic Materials*, **38**, 691 (2009). Doi: <https://doi.org/10.1007/s11664-008-0636-8>
  15. D. Q. Yu, W. Jillek and E. Schmitt, Electrochemical migration of Sn-Pb and lead free solder alloys under distilled water, *Journal of Materials Science: Materials in Electronics*, **17**, 219 (2006). Doi: <https://doi.org/10.1007/s10854-006-6764-0>
  16. X. He, M. H. Azarian and M. G. Pecht, Evaluation of electrochemical migration on printed circuit boards with lead-free and tin-lead solder, *Journal of Electronic Materials*, **40**, 1921 (2011). Doi: <https://doi.org/10.1007/s11664-011-1672-3>
  17. G. Hars'anyi, Irregular effect of chloride impurities on migration failure reliability: contradictions or understandable?, *Microelectronics Reliability*, **39**, 1407 (1999). Doi: [https://doi.org/10.1016/S0026-2714\(99\)00079-7](https://doi.org/10.1016/S0026-2714(99)00079-7)
  18. X. Shi, G. Hansen, M. Mills, S. Jungwirth and Y. Zhang, Preserving the value of highway maintenance equipment against roadway deicers: a case study and preliminary cost benefit analysis, *Anti-Corrosion Methods and Materials*, **63**, 1 (2016). Doi: <https://doi.org/10.1108/ACMM-07-2014-1410>
  19. N. K. Othman, F. R. Omar and F. C. Ani, Electrochemical migration and corrosion behaviours of SAC305 reinforced by NiO, Fe<sub>2</sub>O<sub>3</sub>, TiO<sub>2</sub> nanoparticles in NaCl solution, *IOP Conference Series: Materials Science and Engineering*, **701**, 012044 (2019). Doi: <https://doi.org/10.1088/1757-899X/701/1/012044>
  20. P. Yi, Kui Xiao, K. Ding, C. Dong and X. Li, Electrochemical Migration Behavior of Copper-Clad Laminate and Electroless Nickel/Immersion Gold Printed Circuit Boards under Thin Electrolyte Layers, *Materials*, **10**, 137 (2017). Doi: <https://doi.org/10.3390/ma10020137>
  21. B. Medgyes, A. Gharaibeh, G. Harsányi, B. Pécz, I. Felhősi, Electrochemical corrosion and electrochemical migration characteristics of SAC-1Bi-xMn solder alloys in NaCl solution, *Corrosion Science*, **213** 110965 (2023). Doi: <https://doi.org/10.1016/j.corsci.2023.110965>
  22. S. B. Lee, M. S. Jung, H. Y. Lee, T. Kang and Y. C. Joo, Effect of bias voltage on the electrochemical migration behaviors of Sn and Pb, *IEEE Transactions on Device and Materials Reliability*, **9**, 483 (2009). Doi: <https://doi.org/10.1109/TDMR.2009.2026737>
  23. J. A. Jachim, G. B. Freeman and L. J. Turbini, Use of surface insulation resistance and contact angle measurements to characterize the interactions of three water soluble fluxes with FR-4 substrates, *IEEE Transactions on Components, Packaging and Manufacturing Technology, Part A*, **20**, 443 (1997). Doi: <https://doi.org/10.1109/96.641513>
  24. E. L. Lee, A. S. M. A. Haseeb, W. J. Basirun, Y. H. Wong, M. F. M. Sabri and B. Y. Low, In-situ study of electrochemical migration of tin in the presence of bromide ion, *Scientific Reports*, **11**, 15768 (2021). Doi: <https://doi.org/10.1038/s41598-021-95276-0>
  25. X. Liao, F. Cao, L. Zheng, W. Liu, A. Chen, J. Zhang and C. Cao, Corrosion behavior of copper under chloride

- containing thin electrolyte layer, *Corrosion Science*, **53**, 3289 (2011). Doi: <https://doi.org/10.1016/j.corsci.2011.06.004>
26. C. W. See, M. Z. Yahaya, H. Haliman, A. A. Mohamad, Corrosion Behavior of Corroded Sn-3.0Ag-0.5Cu Solder Alloy, *Procedia Chemistry*, **19**, 847 (2016). Doi: <https://doi.org/10.1016/j.proche.2016.03.112>
27. IPC-TM-650 2.6.14.1 Electrochemical Migration Resistance Test, <http://ipc.org> (2000).